IOPscience iopscience.iop.org

Home Search Collections Journals About Contact us My IOPscience

Possibility of reverse Monte Carlo modelling for hydrogenated amorphous Si deposited on reactive ion etched Si substrate

This article has been downloaded from IOPscience. Please scroll down to see the full text article.

2007 J. Phys.: Condens. Matter 19 335211

(http://iopscience.iop.org/0953-8984/19/33/335211)

View the table of contents for this issue, or go to the journal homepage for more

Download details:
IP Address: 129.252.86.83
The article was downloaded on 28/05/2010 at 19:59

Please note that terms and conditions apply.

IOP Publishing — Journal of Physics: Condensed Matter

J. Phys.: Condens. Matter **19** (2007) 335211 (9pp) doi:10.1088/0953-8984/19/33/335211

Possibility of reverse Monte Carlo modelling for hydrogenated amorphous Si deposited on reactive ion etched Si substrate

Toshio Kawahara[1], **Yoshinori Matsui**[1], **Seiichi Tagawa**[1], **Tomoji Kawai**[1] **and Hideki Matsumura**[2]

[1] The Institute of Scientific and Industrial Research, Osaka University, 8-1 Mihogaoka 567-0047, Japan
[2] School of Materials Science, Japan Advanced Institute of Science and Technology, Ishikawa 923-1292, Japan

E-mail: toshi@sanken.osaka-u.ac.jp

Received 9 February 2007
Published 4 July 2007
Online at stacks.iop.org/JPhysCM/19/335211

Abstract
We examined the x-ray diffraction (XRD) patterns of hydrogenated amorphous Si (a-Si:H) and of crystalline Si (c-Si) substrate for high-Q measurements. A structural analysis of thin films on substrates is important for the development of real devices. A transmission geometry with high-energy x-rays was used for this investigation, together with very thin substrates, in an effort to reduce substrate signals. A small area of the substrate was etched using the reactive ion etching (RIE) plasma process to maintain free-standing structures, and a-Si was deposited using catalytic chemical vapour deposition techniques. The x-ray beam was focused on the processed area and a-Si diffraction using a thin Si layer was measured. Unlike a-Si:H films on substrates without etching, we succeeded in detecting amorphous signals from samples deposited on the processed substrate. Application of reverse Monte Carlo (RMC) modelling using these data and subtracting Si substrate peaks was investigated. Direct subtraction and MCGR program (Pusztai and McGreevy 1997 *Physica* B **234–236** 357–8) normalization for the ratio estimation between c-Si and a-Si:H structure factors was employed. MCGR normalization was found to improve subtraction of the c-Si peaks and the first peak at $r = 2.3$ in the pair distribution function $g(r)$ could be calculated.

(Some figures in this article are in colour only in the electronic version)

1. Introduction

In current thin film devices, the integrated circuit (IC) is fabricated following application of various thin film processes. For example, amorphous Si (a-Si) films are widely used for

devices such as thin film transistors and solar cells. Hydrogenated amorphous Si (a-Si:H) is usually prepared by plasma enhanced chemical vapour deposition (PECVD) using silane (SiH_4) gas [1–3]. On the other hand, catalytic chemical vapour deposition (cat-CVD) has been considered a superior technique for the production of a-Si:H required for practical applications. Cat-CVD grown a-Si:H exhibits stability which seems to be derived from the low content (a few at.%) of hydrogen in a-Si:H [4–6]. These two deposition methods can generate different structures in a-Si:H, and large stress in a-Si deposited by PECVD has been reported [7].

For this purpose, analysis using a three-dimensional (3D) structure seems to be important. The use of sturdy materials with well-established device parameters is required for future high-performance devices, and amorphous materials generally possess structural freedom that can generate a variety of atomic configurations in the materials. Conventional techniques for structural analysis employ the pair distribution function $g(r)$ as the 1D information. Experimental data pertaining to electron diffraction [8], high-energy x-ray diffraction [9], x-ray absorption [10] and neutron diffraction [11] were used for the structural analysis of a-Si. From a theoretical standpoint, a model structure for a-Si has been established using a traditional Monte Carlo simulation [12] and first principles calculations [13, 14]. To obtain a 3D structure, interatomic potentials are usually required and the general potential may yield a structure that differs from that of the actual material.

Reverse Monte Carlo (RMC) modelling represents one experimental technique which provides a 3D model of an individual sample without use of any hypothesis relating to interatomic potential [15–18], and it is particularly suited to dense solids and liquids. RMC analysis has been applied to H-free a-Si in the study of microscopic structures by Kugler *et al* [16]. They initially compared neutron data to conventional theoretical models [19]. In the amorphous case there is some ambiguity and other constraints for the simulation are required. For H-free a-Si, unusual atomic arrangements have been revealed by RMC simulation [20, 21]. RMC modelling was also used in the case of hydrogenated a-Si:H with low H content [22, 23] and comparisons made between a-Si:H films deposited by cat-CVD with those deposited by PECVD [7].

However, high-Q data are required in the structure factor $S(Q)$ for the modelling. X-ray diffraction (XRD) is a powerful technique in structural analysis where only small amounts of material are required in comparison to other methodologies such as the use of neutron diffraction. The use of high-energy x-rays has revealed the structure of bulk materials such as liquid germanium [24]. Ion-implanted a-Si was studied by XRD at an extended Q range [9, 25]. XRD can be applied to a-Si thin films deposited on Si substrates using x-rays with low incident angle [26]. However, when the energy of the x-rays increases, the penetrating power of the x-rays prohibits high-Q measurements of thin film samples, where substrate signals mask the main signals from the thin films.

One possible way to obviate this problem in experiments utilizing thin films is by removal of the substrate. However, given that real sample structures are dependent on the substrate, structural analysis of thin film samples should be performed on substrates. Furthermore, accurate measurement of diffraction signals of a thin film on a substrate remains problematic. Consequently, we tried to measure the XRD patterns of a-Si:H with Si substrate in high Q measurements. Very thin substrate was used, to reduce the substrate signals. A small area of the substrate was etched using a plasma process in an effort to maintain free-standing structures, and then the a-Si was deposited on the processed substrate using cat-CVD techniques. The x-ray beam was focused on the etched area and a-Si diffraction with a thin Si layer was measured.

Samples were fabricated for dry processing using reactive ion plasma. The dry process has recently been used in the etching process given advantages concerning waste and control of etching. There are several high-density techniques available such as electron cyclotron

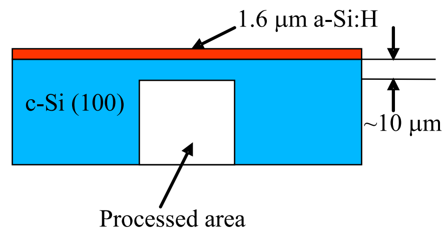

Figure 1. Schematic of a fabricated sample structure. X-rays were focused on the processed area.

resonance or inductively coupled plasma [27]. However, conventional reactive ion etching (RIE) was chosen since it is very useful when applied to Si-related materials with a slightly slow etching rate. Mechanical polishing using a diamond drill was employed to shorten the processing time.

In the diffraction pattern for a-Si:H deposited on the Si substrate without etching, only signals derived from the Si substrate are observed since the tail of the Si peaks masks the diffraction from a-Si. In contrast, amorphous signals derived from samples deposited on processed substrates were successfully detected. In this paper, a structural analysis of a-Si:H thin films deposited on processed substrates is presented. The diffraction data of a-Si:H with crystal substrate signals are used and constraints concerning coordination number seem to be very important. The Fourier transform infrared (FTIR) spectra of a-Si films were measured and coordination number constraints estimated.

2. Experiments and analysis

The crystal Si (c-Si) (100) substrate was thinned to 100 μm with area 1.2×0.8 mm^2 using a diamond drill. The thickness of the starting Si substrate was 500 μm. The RIE process employed followed the diamond drill process. During etching, the surface, which was used for film deposition, was protected by ZEP-520 (Zeon) resist. Etching was performed with a CF_4 and Ar gas flow of 80 and 15 standard cubic centimetres/minute (sccm), respectively, and an RF power of 150 W. The pressure in the process chamber was 30 Pa. Under these conditions, the etching rate of the RIE process for Si was 3.0 μm h^{-1}. The backside of the Si was etched to slight transparency: the thickness might have been less than 10 μm with surface roughness $R_a \sim 0.3$ μm. Approximately 10 μm with a free-standing area of 1.2×0.8 mm^2 was achieved for the substrate.

The a-Si:H films were deposited by cat-CVD on a Si(100) wafer by RIE. The same deposition conditions were employed as those described for device quality a-Si:H films using the cat-CVD device fabrication proposed by Sakai *et al* [5]. The H content and density of the a-Si:H films were 2% and 2.28 g cm^{-3}, respectively, and these values were used for the modelling parameters in the RMC calculation. In an effort to obtain large signals from the thin films, thick a-Si:H films were fabricated to 1.6 μm. A schematic of the fabricated sample structure is shown in figure 1. The film to substrate ratio for x-ray measurements was significantly improved by the etching process. As a comparison, a-Si:H films on a thick substrate without etching (sample 2) and a c-Si substrate etched by RIE (sample 3) were used (table 1).

For estimation of the ratio of Si–H and Si–H_2, Fourier transform infrared (FTIR) spectra recorded by a Shimadzu FT-IR 8300 FTIR spectrometer were used (figure 2). Experimental data was subjected to Gaussian fitting and the splitting of two peaks corresponded to the Si–H bond stretching mode. Thus we observed the Si–H and Si–H_2 stretching modes at 2000 and 2100 cm^{-1}, respectively. The ratio of the two areas was Si–H:Si–H_2 = 9.02:1, and using the

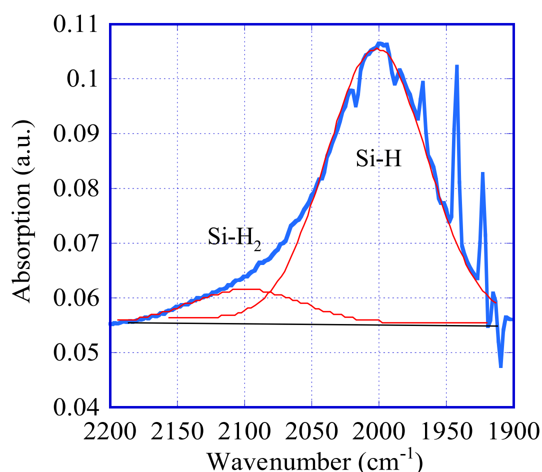

Figure 2. FTIR spectra of cat-CVD-deposited a-Si:H films. The H content is 2%. Two absorption peaks for Si–H (2000 cm^{-1}) and $Si–H_2$ (2100 cm^{-1}) are shown. The curves were calculated by Gaussian fitting.

Table 1. Sample list.

a-Si thickness (μm)	Substrate thickness (μm)	Sample number
1.6	~10	Sample 1
1.6	500	Sample 2
0	~10	Sample 3

proportional constant (A-values) for the stretching mode [28], we estimated the ratio of Si–H and $Si–H_2$ as 1.56% and 0.4%, respectively.

X-ray diffraction measurements for $S(Q)$ were performed at the high-energy line BL04B2 at SPring-8 (JASRI) [29]. The energy of the x-rays was 61.52 keV and the Q range scanned was from 0.5 to 20.5 $Å^{-1}$. X-rays were focused to the processed area with a beam size of 0.5 mm^2.

RMC is a well-established simulation method that can be applied to three-dimensional atomic structures [17, 18]. Here we used a cubic configuration comprising 4096 atoms ($16 \times 16 \times 16$ atoms) with a 43.6 Å cubic lattice in real space. Since the structure of a-Si is thought to be similar to that of c-Si, the crystal structure of c-Si was selected as the initial configuration for the calculation. Generally, the empirical three-body potential is known to be better for Si [30]. For simplicity, however, the minimum interatomic distance between Si atoms was set as 2.095 Å as estimated by the Lennard-Jones interaction, where the χ^2 of the RMC calculation is the minimum. Assignment of constraints is important in the simulation since RMC modelling involves many possible structures. The diffraction data of a-Si:H including the crystal substrate signals was assessed and the estimated ratio of Si–H and $Si–H_2$ was used for the coordination number constraint in the modelling.

3. Results and discussion

The XRD patterns for a-Si:H deposited on the non-processed (sample 2) and processed (sample 1) substrates, where the Si thickness for the measured area differed (500 and ca. 10 μm,

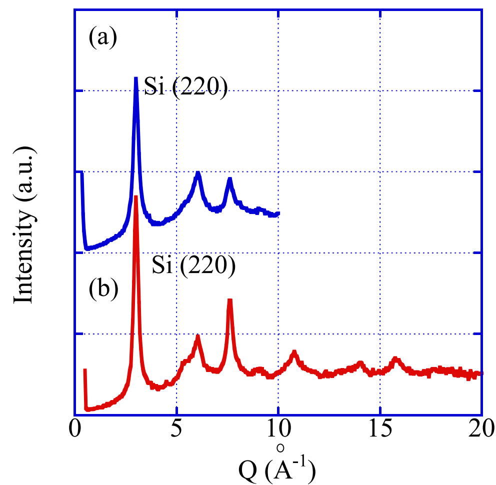

Figure 3. Experimental XRD patterns of samples 2 and 3. (a) Sample 2 represents a-Si:H films deposited on non-processed substrate. (b) Sample 3 represents c-Si substrate that was processed and used in the simulation.

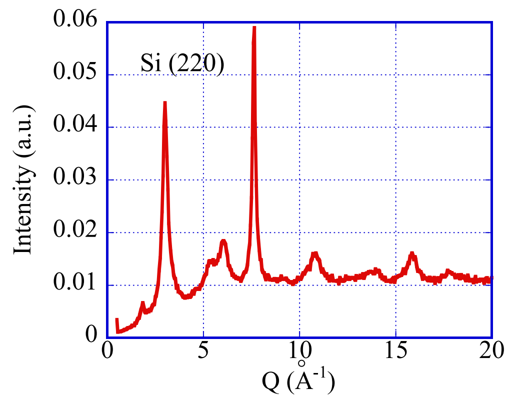

Figure 4. Experimental XRD pattern of a-Si:H deposited on processed substrate (sample 1).

respectively), are shown in figures 3(a) and 4, respectively. Only the c-Si peaks can be observed for sample 2, as shown in figure 3(a). The c-Si (220) peak manifests as the first peak for c-Si. Figure 3(b) shows $S(Q)$ for single-crystal Si etched by the RIE process (sample 3), whose thickness was about 10 μm. This XRD pattern is almost the same as that shown in figure 3(a). The substrate in sample 3 might have been damaged during plasma etching, which would account for the observed diffuse scattering [31] in the XRD pattern. However, the pattern appears to resemble the XRD pattern of sample 2 and so any damage present might be small. It is also important to measure the substrate XRD patterns using the same substrate as that used to deposit the sample on.

In contrast to these XRD patterns, figure 4 shows several peaks related to the presence of amorphous materials in the $S(Q)$ of a-Si:H (sample 1). Thus, amorphous peaks can be observed for thin film samples with the substrate at the transmission geometry. Following previous reports related to cat-CVD-grown a-Si:H [22, 23], clear peaks can be observed which

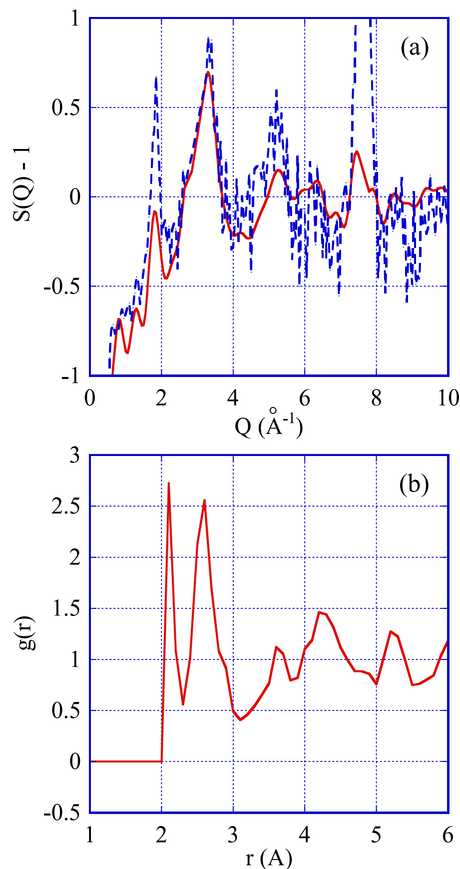

Figure 5. Structure factor $S(Q)$ obtained by RMC modelling in (a) and calculated pair distribution function $g(r)$ in (b). Subtraction of substrate peaks by direct ratio estimation between a-Si:H and c-Si (220). The dotted line represents experimental $S(Q)$ and the solid line that for RMC modelling in (a).

are related to a-Si:H at $Q = 1.95$ and the shoulders ($Q = 5.7$ and 6.7) of a-Si:H of the peak around $Q = 6.0$. The shoulder at $Q = 8.2$ might relate to a-Si:H, although the c-Si peak is very large. There is also a small peak at $Q = 8.8$ for a-Si:H. These peaks are similar to those observed for evaporated a-Si [32]. The second a-Si peak at $Q = 3.6$ is hard to differentiate due to the crystal peak. Thus, crystal peaks generate error in the structural analysis. An attempt was made to subtract the crystal peaks from the experimental data.

Initially, direct subtraction was employed in an effort to subtract the crystal peak between the amorphous $S(Q)$ and Si substrate. The ratio was calculated from the ratio of the (220) peak of c-Si for samples 1 and 3. The resulting $S(Q)$ was modeled by the `RMCA` program with the coordination number constraint. The calculated $S(Q)$ is shown in figure 5(a). Calculated values for the first peak of the structure factor decreased, while the second peaks are too wide in comparison to $S(Q)$ of a-Si:H measured by Seemann–Bohlin methods [23]. Although the large peak around $Q = 7.5$ decreased in the simulation, it still appeared too large given the large second peak of c-Si in the experimental data. In this case, the first $g(r)$ peak is just above 2.0, which is too small, as shown in figure 5(b). However, there is no peak around $r = 3$, one clear advantage in employing this direct subtraction. In an effort to reduce the

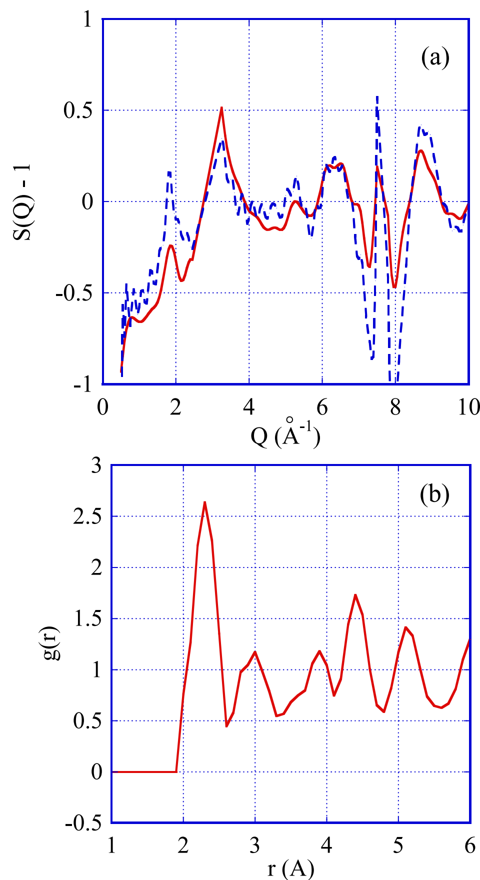

Figure 6. Structure factor $S(Q)$ obtained by RMC modelling in (a) and calculated pair distribution function $g(r)$ in (b). The ratio of the substrate peaks was estimated by MCGR normalization. The dotted line represents experimental $S(Q)$ and the solid line that for RMC modelling in (a).

contribution by the second c-Si peak, an attempt was made to delete the second large crystal Si peak ($Q \sim 7.5$) in the experimental $S(Q)$. It was believed that this second peak should improve following experimental improvements, such as using the $S(Q)$ of the same substrate as used in the deposition. The calculated $g(r)$ for direct subtraction without the second c-Si peak improved slightly; the first peak of $g(r)$ shifted slightly to larger r, whose values were closer to the ones measured with low-angle incident beam geometry.

The experimental $S(Q)$ was then normalized using by the MCGR program [33], which represents the Monte Carlo program involving inverse methods, and the crystal peaks were subtracted from the a-Si:H diffraction with substrate. The ratio for the subtraction was calculated by the ratio of the c-Si (220) peaks. This $S(Q)$ is plotted in figure 6(a). Although the large second peak was present in the modified diffraction data, just as with the direct subtraction method, the normalized second peak became smaller. The calculated first peak in $S(Q)$ is small in figure 6(a) given the increased width of the second peak in $S(Q)$ related to the remainder of the crystal peaks. However, several amorphous peaks can be seen in the structure factor. The $g(r)$ calculated by rmca is shown in figure 6(b). In contrast to direct subtraction, the first peaks of $g(r)$ shifted to higher r values, and the first peak in $g(r)$ is at $r = 2.3$ and seems improved [23]. The peak at $r = 3.9$ is also observed in $g(r)$ of the

MCGR subtraction. Compared to evaporated a-Si, similar peaks at $r = 2.3$, 3.9 and 4.3 were observed [32]. Therefore it is believed that RMC modelling is improved following MCGR normalization. However, one disadvantage relates to the presence of the peak at $r = 3$ in $g(r)$. Deletion of the second c-Si peak ($Q \sim 7.5$) in the $S(Q)$ was also attempted. The $g(r)$ around $r = 3$ slightly decreased in comparison to $g(r)$ with the second c-Si peak. The first peak and the peak at $r = 3.9$ is also observed in $g(r)$ without the c-Si second peak in $S(Q)$. Omission of the second large c-Si peak yielded no apparent improvements except for a small decrease in a peak in $g(r)$ at around $r = 3$. On the other hand, the $S(Q)$ data below the large second c-Si peak could be used, but they seemed to be too short.

The amorphous peaks could be observed in the $S(Q)$ measured at the transmission geometry. However, there are many unusual peaks in the amorphous $g(r)$. These errors are caused by the difference between the crystal peaks of the measured substrate and that of the film samples. This highlights the importance of a suitable $S(Q)$ of the substrate for the amorphous films. For further improvement, measurement of the Si substrate prior to film deposition represents one key experiment. The reproducibility of $S(Q)$ at SPring-8 is very good. It is believed that measurement of the same substrate using film deposition can solve the problem of estimating the substrate $S(Q)$. These experiments are now in progress. In this context, we can succeed in direct measurement of thin film structure factors with a processed substrate.

4. Conclusion and future prospects

We have succeeded in the direct measurement of a-Si deposited on Si substrate in the transmission geometry required for a wide Q range. In the measured data, the diffraction peaks from the Si substrate mask the amorphous peaks. Plasma etching was used for thinning the Si substrate to enhance diffraction from the thin films. To estimate the c-Si peaks for the subtraction, a direct ratio calculation of the first c-Si (220) peak and MCGR normalization were used. Compared with direct subtraction, MCGR can improve estimation of the c-Si peaks. Following this, the first peak in $g(r)$ was observed at around $r = 2.3$.

Further improvement in the separation between c-Si and a-Si:H signals seems to be necessary. Use of a SiO_2 thin layer could improve substrate background peaks that do not possess large Bragg peaks. In this case, use could be made of the wet process since the SiO_2 layer can be used as a stopping layer. Every effort should be made to select a substrate that is appropriate to the thin film in question. Precise estimation of the c-Si peaks is required in order to improve the simulations. Use of XRD pattern data of the same substrate as that employed for film deposition represents the most promising improvement. The backside Si layer thickness dependence of the diffraction pattern can assist in the estimation of c-Si signals and could improve the modelling.

Acknowledgments

We acknowledge the help of Dr S Kohara of JASRI for the x-ray diffraction measurements at SPring-8. X-ray diffraction measurements were performed with the JASRI and Proposal Number 2005B-0203. Dr N Tabuchi and Mr M Fukuda of JAIST helped with the sample preparation by cat-CVD. Portions of the experimental work were supported by the nanotechnology support project of the Ministry of Education, Culture, Sports, Science and Technology (MEXT), Japan. MEXT also supported us as the Creation of Innovation Centers for Advanced Interdisciplinary Research Areas.

References

[1] Matsuda A and Tanaka K 1982 *Thin Solid Films* **92** 171
[2] Irrera F 1994 *J. Appl. Phys.* **75** 1396
[3] Kobayashi H, Kasama Y, Fujinaga T, Takahashi M and Koinuma H 2002 *Solid State Commun.* **123** 151
[4] Mahan A H, Carapella J, Nelson B P, Crandall R S and Balberg I 1991 *J. Appl. Phys.* **69** 6728
[5] Sakai M, Tsutsumi T, Yoshioka T, Masuda A and Matsumura H 2001 *Thin Solid Films* **395** 330
[6] Mahan A H, Williamson D L, Nelson B P and Crandall R S 1989 *Phys. Rev.* B **40** 12024
[7] Tabuchi N, Kawahara T, Arai T, Morimoto J and Matsumura H 2005 *Japan. J. Appl. Phys.* **44** 3808
[8] Barna A, Barna P B, Radnoczi G, Tóth L and Thomas P 1977 *Phys. Status Solidi* a **41** 81
[9] Laaziri K, Kycia S, Roorda S, Chicoine M, Robertson J L, Wang J and Moss S C 1999 *Phys. Rev.* B **60** 13520
[10] Cicco A D, Bianconi A, Coluzza C, Rudolf P, Lagarda P, Flank A M and Marcelli A 1990 *J. Non-Cryst. Solids* **116** 27
[11] Fortner J and Lannin J S 1989 *Phys. Rev.* B **39** 5527
[12] Wooten F, Winer K and Weaire D 1985 *Phys. Rev. Lett.* **54** 1392
[13] Stich I, Car R and Parrinello M 1991 *Phys. Rev.* B **44** 11092
[14] Orita N, Matsumura T and Katayama-Yoshida H 1996 *J. Non-Cryst. Solids* **192–200** 347
[15] Evrard G and Pusztai L 2005 *J. Phys.: Condens. Matter* **17** S1
[16] Kugler S, Pusztai L, Rosta L, Chieux P and Bellissent R 1993 *Phys. Rev.* B **48** 7685
[17] McGreevy R L and Pusztai L 1988 *Mol. Simul.* **1** 359
[18] McGreevy R L 2001 *J. Phys.: Condens. Matter* **13** R877
[19] Kugler S, Molnár G, Petö G, Zsoldos E, Rosta L, Menelle A and Bellissent R 1989 *Phys. Rev.* B **40** 8030
[20] Várallyay Z and Kugler S 2002 *J. Non-Cryst. Solids* **299–302** 265
[21] Kugler S, Kohary K, Kádas K and Pusztai L 2003 *Solid State Commun.* **127** 305
[22] Tabuchi N, Kawahara T, Arai T, Morimoto J and Matsumura H 2004 *Japan. J. Appl. Phys.* **43** 6873
[23] Kawahara T, Tabuchi N, Arai T, Sato Y, Morimoto J and Matsumura H 2005 *J. Phys.: Condens. Matter* **17** S103
[24] Kawakita Y, Fujita S, Kohara S, Ohshima K, Fujii H, Yokota Y and Takeda S 2005 *Nucl. Instrum. Methods Phys. Res.* B **238** 129
[25] Laaziri K, Kycia S, Roorda S, Chicoine M, Robertson J L, Wang J and Moss S C 1999 *Phys. Rev. Lett.* **82** 3460
[26] Matsubara E, Waseda Y and Itozaki H 1988 *Trans. JIM* **28** 1
[27] Kawahara T, Fälth F, Xinyu L, Nunes R, Andersson T G, Desmaris V, Zirath H, Paskov P P and Holtz P O 2004 *Proc. 3rd Int. Conf. on Materials Processing for Properties and Performance (Singapore, November 24–26 2004) (MP^3)* vol 2, ed K A Khor, R V Ramanujan, C P Ooi and J Zhao p 548
[28] Langford A A, Fleet M L, Nelson B P, Lanford W A and Maley N 1992 *Phys. Rev.* B **45** 13367
[29] Kohara S, Suzuya K, Kashihara Y, Matsumoto N, Umesaki N and Sakai I 2001 *Nucl. Instrum. Methods Phys. Res.* A **467/468** 1030
[30] Stillinger F H and Weber T A 1985 *Phys. Rev.* B **31** 5262
[31] Gronkowski J and Borowski J 2001 *Cryst. Res. Technol.* **36** 815
[32] Pusztai L and Kugler S 2005 *J. Phys.: Condens. Matter* **17** 2617
[33] Pusztai L and McGreevy R L 1997 *Physica* B **234–236** 357